COMBINED CONTROL-STRUCTURE OPTIMIZATION

M. Salama, M. Milman, R. Bruno, R. Scheid
Jet Propulsion Laboratory
California Institute of Technology

S. Gibson
University of California, Los Angeles

1. INTRODUCTION

The strong interaction between structural dynamics and active control is a well-recognized challenge in the analysis of controlled flexible structures. But it is only recently that the same interaction has been exploited in the design process. The traditional design approach in which the control design comes very late in the development — typically after the structure has been designed and built — is no longer viable. Although this approach has produced satisfactory results for the attitude control of relatively rigid space structures, it will not be suitable for the ambitious space missions that require precise controlled pointing of telescopes, interferometers and the vibration suppression for science instruments mounted on large flexible structures. In such systems, designing the structure and designing its control become entwined. This dictates early consideration of the control design — well before any detailed structural design is finalized. And just as the structure is optimally designed to meet such performance metrics as minimum mass or response to external disturbances, it should be optimally designed to meet its ultimate control performance as well.

A natural way to introduce the control element into the overall design process is through an optimization procedure that combines the structural and control design criteria into a single problem formulation. A number of authors [1-6] have taken this perspective. In terms of the types of design parameters and constraints considered, Ref. (2) is probably the most extensive in that the design variables include structure parameters, actuator locations and feedback matrix. Static output feedback is used, and the performance objectives include total mass and robustness measures. Constraints are imposed on the eigenvalue placements, performance bounds, and structural constraints. Since not all of the constraints are commensurate, they are relaxed using a homotopy approach. Just as with Ref. (6), the approach taken in the present paper is not to produce the "best" optimized point design, but to produce a family of Pareto optimal designs representing options that assist in early trade studies. The philosophy is that these are candidate designs to be passed on for further consideration, and their function is more to guide the system design rather than to represent the ultimate design.

An optimization approach that is consistent with this philosophy is to utilize multiple cost objectives that include an LQG cost criterion in conjunction with structural cost(s), and possibly other control related costs.

After introducing the combined objective formulation in the setting of vector optimization, we derive the necessary conditions for Pareto optimality. No behavioral constraints are explicitly imposed in the problem formulation and a homotopy approach is used to generate a family of optimum designs. The intent of this paper is to explore this design approach and to provide an exposition of the computational aspects of the problem using numerical examples.

2. COMBINED OPTIMIZATION

The combined optimization approach can be best appreciated when contrasted with the traditional sequential optimization. In the sequential optimization, the structure is first optimized by selecting the design variable, α (e.g. member sizes) which minimize a structural criterion $J_s(\alpha)$ - often taken as the mass of the structure subject to some behavioral constraints $h(\alpha)\geq 0$ on deformations, stresses, open-loop frequencies, etc.

$$\min_{\alpha} J_s(\alpha) \; ; \qquad h(\alpha)\geq 0, \; \alpha \epsilon D \tag{2.1}$$

where D is the physical domain for α. Second, having completely specified the optimal structural design α^*, the control optimization is carried out with α^* fixed. For example, LQG or H_∞ optimal control designs pose the problem:

$$\min_{C} J_c(\alpha^*, C) \tag{2.2}$$

where J_c represents either of the control criterion, and C is allowed to vary over the class of stabilizing compensators for the plant.

By contrast, in the combined optimization formulation, the goal is to first merge the criteria of interest (here J_s and J_c) into one using non-negative multipliers β, and δ, then optimize the combined criterion over the original design variable space α, C:

$$\min_{\alpha, C} [\beta J_s(\alpha) + \delta J_c(\alpha, C] \tag{2.3}$$

The following expression compares the results of the two optimization procedures outlined above.

$$\min_{\alpha, C} [\beta J_s(\alpha) + \delta J_c(\alpha, C)] \leq [\min_{\alpha} \beta J_s(\alpha) + \min_{C} \delta J_c(\alpha^*, C)] \tag{2.4}$$

The right-hand side of (2.4) corresponds to performing the sequential optimization by solving (2.1) for α^*, followed by solving (2.2) for C*. Note that the optimal solution of the right-hand side is independent of β and δ- but not so for the combined optimization embodied by the left-hand side. In terms of the total cost, expression (2.4) states the fact that the combined optimization is never inferior to the sequential optimization. In the vector optimization setting, the relative weighting of β and δ serves as a parameter that allows the generation of an entire family of Pareto optima.

In the present paper, only two objective criteria are dealt with. But it is not difficult to generalize the approach to incorporate other criteria such

as minimum open-loop frequency and certain controller robustness measures. In general these criteria are noncommensurate, and there is no unique solution that minimizes all criteria $J_1,\ldots,J_N$ simultaneously. Thus, one must look for Pareto optimal solutions as outlined below.

First one assembles the criteria $J_i:D\to R$, $i=1,\ldots,N$ into a single criterion $J:D\to R^N$, $J(\alpha)=(J_1(\alpha),\ldots,J_N(\alpha))^T$. Then the cone $C_o = \{x\epsilon R^N: x_i\geq 0,\ i=1,\ldots,N\}$ is defined to induce a partial ordering $\leq$ on R^N by $x\leq y$ if $y-x\ \epsilon C_o$. Now let $\alpha\epsilon D$. A design vector $\alpha^*\epsilon D$ is said to be (strongly) Pareto optimal if $J(\alpha)\leq J(\alpha^*)$ implies $J(\alpha)=J(\alpha^*)$. A necessary condition for Pareto optimality is contained in the following theorem due to Lin [7].

Theorem 2.1: If α^* is Pareto optimal for the combined criterion J, and D is an open set, then there exists a nonzero vector $Z\epsilon C_o$ such that $Z^T J_*(\alpha^*)=0$. Here J_* denotes the differential of J.

For the two-term optimization problem in (2.3), we find that the Pareto optimal solution to $J = (J_s,\ J_c)^T$ can be generated by solving for the necessary conditions for extremizing the following convex combination J_λ:

$$J_\lambda = (1-\lambda)\ J_s(\alpha) + \lambda J_c(\alpha,C);\quad \lambda\epsilon[0,1] \tag{2.5}$$

where λ replaces β, δ in (2.3). The form of Eq. (2.5) suggests a homotopy (or continuation) approach for generating a family of Pareto optima as λ is propagated from 0 to 1.

3. NECESSARY CONDITIONS

We begin with the n_s degree-of-freedom dynamical system

$$M(\alpha)\ddot{r} + D(\alpha)\dot{r} + K(\alpha)r = G_1u + G_2\upsilon \tag{3.1}$$

where M, D, and K are the $n_s x n_s$ mass, damping and stiffness, G_1 is the constant $n_s x n_u$ control influence matrix, and G_2 is the constant $n_s x n_d$ disturbance matrix. The vectors r, u, and υ are respectively, physical degrees-of-freedom, control forces and disturbances. Let $x = (r,\dot{r})^T$. Then the first order state equation is

$$\dot{x} = A(\alpha)x + B_1(\alpha)u + B_2(\alpha)\ \upsilon + \upsilon' \tag{3.2}$$

where

$$A = \begin{bmatrix} 0 & I \\ -M^{-1}K & -M^{-1}D \end{bmatrix},\quad B_1 = \begin{bmatrix} 0 \\ M^{-1}G_1 \end{bmatrix},\quad B_2 = \begin{bmatrix} 0 \\ M^{-1}G_2 \end{bmatrix} \tag{3.2a}$$

and an additional disturbance υ' independent of α has been introduced for greater flexibility of the formulation. We assume that (3.2) has measured output variables y and controlled output variables z:

$$\begin{aligned} y &= C_1x + w, \\ z &= C_2x \end{aligned} \tag{3.3}$$

and that v, v', and w are uncorrelated white noise processes with intensities Q_v, V, and Q_w, respectively.

In the remainder of this paper, the total mass of the structure is assumed to represent the structural criterion J_s. Thus, for a structure consisting of n_a one-dimensional finite elements, each having a cross-sectional area α_i, length ℓ_i and density ρ:

$$J_s = \sum_i^{n_a} \rho \ell_i \alpha_i \tag{3.4}$$

For the control criterion J_c associated with (3.2) and (3.3), we assume the LQG index

$$J_c = \lim_{t\to\infty} E\{z^T(t)\bar{D}z(t) + x^T D_1 x + u^T(t)Ru(t)\} \tag{3.5}$$

where E is the expectation, $\bar{D}$ and D_1 are non-negative definite weighting matrices, and R is positive definite. Although D_1 is assumed independent of α, D could possibly depend on α. The latter case would arise, for instance, if the first term in (3.5) were to represent the total energy in the system with $z = (r,\dot{r})^T$ and $D = \mathrm{diag}(K,M)$. Under standard assumptions of stabilizability and detectability, the optimal compensator C* for (3.5) is implemented by [8]:

$$\begin{aligned} u_o &= -B_1^T P x_o \\ \dot{x}_o &= (A-K_f C)x_o + K_f y + B_1 u_o, \end{aligned} \tag{3.6}$$

and the optimal cost J_c associated with this compensator is

$$J_c(C) = \mathrm{tr}\{P(B_2 Q_v B_2^T + V) + P_f P B_1 R^{-1} B_1^T P\}. \tag{3.7}$$

where P and P_f are the unique positive definite solutions to the algebraic Riccati equations

$$\begin{aligned} A^T P + PA + D_o - PB_1 R^{-1} B_1^T P &= 0, \\ AP_f + P_f A^T + B_2 Q_v B_2^T + V - P_f C_1^T Q_w^{-1} C_1 P_f &= 0 \end{aligned} \tag{3.8}$$

and $D_o = C_2^T \bar{D} C_2 + D_1$, and $K_f = P_f C_1^T Q_w^{-1}$

With the above representation for J_c, we seek the optimality conditions for

$$\min_\alpha J_\lambda(\alpha) = (1-\lambda)J_s(\alpha) + \langle \nu, \alpha \rangle + \lambda \mathrm{tr}\{P(B_2 Q_v B_2^T + V) + P_f P B_1 R^{-1} B_1^T P\} \tag{3.9}$$

subject to the constraints in (3.8). In (3.9) an n_a-dimensional vector $\nu \epsilon R^{n_a}$ has been introduced to "regularize" the problem and to serve the purpose of initializing the homotopy path.

Proposition 3.1 Let Σ_+ denote the set of n_x xn_x positive definite matrices. The optimality conditions for α^* to be a local extremum of (3.9) subject to (3.8) are the zeros of the function H: RxR^{na} x Σ_+ x Σ_+ $\rightarrow$ R^{na} x Σ_+ x Σ_+ defined by $H = [H_1, H_2, H_3, H_4, H_5]$, where

$$H_1(\lambda,\alpha,Z_1,Z_2,P,P_f) =$$

$$(1-\lambda)\frac{\partial J_s}{\partial \alpha_i} + \nu_i + \lambda tr\{P \frac{\partial (B_2 Q_v B_2^T)}{\partial \alpha_i} + PP_fP \frac{\partial (B_1 R^{-1} B_1^T)}{\partial \alpha_i} + Z_1[\frac{\partial A^T}{\partial \alpha_i}P + P\frac{\partial A}{\partial \alpha_i} + \frac{\partial D_o}{\partial \alpha_i}$$

$$-P \frac{\partial (B_1 R^{-1} B_1^T)}{\partial \alpha_i} P] + Z_2[\frac{\partial A}{\partial \alpha_i} P_f + P_f \frac{\partial A^T}{\partial \alpha_i} + \frac{\partial (B_2 Q_v B_2^T)}{\partial \alpha_i} - P_f \frac{\partial (C_1^T Q_w^{-1} C_1)}{\partial \alpha_i} P_f]\},$$

$$i=1,\ldots,n_a \qquad (3.10a)$$

$$H_2(\lambda, \alpha, Z_1, Z_2, P, P_f) =$$

$$(A-B_1R^{-1}B_1^TP)Z_1+Z_1(A^T-PB_1R^{-1}B_1^T)+B_2Q_vB_2^T+P_fPB_1R^{-1}B_1^T+B_1R^{-1}B_1^TPP_f \qquad (3.10b)$$

$$H_3(\lambda, \alpha, Z_1, Z_2, P, P_f) =$$

$$(A^T-C_1^TQ_w^{-1}C_1P_f)Z_2+Z_2(A-P_fC_1^TQ_w^{-1}C_1)+PB_1R^{-1}B_1^TP \qquad (3.10c)$$

$$H_4(\lambda, \alpha, Z_1, Z_2, P, P_f) = A^TP+PA+D_o-PB_1R^{-1}B_1^TP, \qquad (3.10d)$$

$$H_5(\lambda, \alpha, Z_1, Z_2, P, P_f) = AP_f+P_fA^T+B_2Q_vB_2^T+V-P_fC_1^TQ_w^{-1}C_1P_f \qquad (3.10e)$$

The proof of proposition (3.1) is omitted here to conserve space, but is given in detail in Ref. [9]. Thus, for the LQG formulation, the necessary conditions involve solving two algebraic Riccati equations (3.10d, e), two Lyapunov equations (3.10b, c), and a gradient equation (3.10a) for α_i, i=1,...,n_a. In

the case of the LQR formulation, it is easily verified that the optimization statement expressed by (3.9) reduces to

$$\min_{\alpha} J_\lambda(\alpha)=(1-\lambda)J_s(\alpha)+\langle\nu,\alpha\rangle+\lambda tr\{P(B_2Q_\upsilon B_2^T+V)\} \tag{3.11}$$

and that the optimality conditions reduce to finding the zeros of the simpler function $H=[H_1, H_2, H_3]$ involving one Riccati and one Lyapunov equation (instead of two as in LQG), in addition to the gradient equations:

$$H_i(\lambda,\alpha,Z,P) = (1-\lambda)\frac{\partial J_s}{\partial \alpha_i} + \nu_i + \lambda tr\{P\frac{\partial (B_2Q_\upsilon B_2^T)}{\partial \alpha_i}$$

$$+Z[2P\frac{\partial A}{\partial \alpha_i}+\frac{\partial D_o}{\partial \alpha_i} - P\frac{\partial (B_1R^{-1}B_1^T)}{\partial \alpha_i}P]\}; \quad i=1,\ldots,n_a \tag{3.12a}$$

$$H_2(\lambda,\alpha,Z,P) = A_cZ + ZA_c^T + B_2Q_\upsilon B_2^T + V, \tag{3.12b}$$

$$H_3(\lambda,\alpha,Z,P) = A^TP + PA + D_o - PB_1R^{-1}B_1^TP, \tag{3.12c}$$

with $A_c = A - B_1R^{-1}B_1^TP$.

4. HOMOTOPY STRATEGY

For all $\lambda\epsilon[0,1]$, our goal is to minimize (3.9) in the case of the LQG formulation or (3.11) in the case of the LQR formulation by finding the design variables α that satisfy the corresponding optimality conditions (3.10) or (3.12). The basic strategy is: given the solution at a value λ_o, smoothly propagate it to a new solution at $\lambda_o+\Delta\lambda$ via some local mechanism such as Newton method or iterative optimization. This strategy has been analyzed in detail in Ref. (9). In the following, only a summary of the results is given without proofs, assuming the LQR formulation.

Let x denote a generic point $(\alpha, Z, P)\epsilon R^{n_a}x \sum_+ x \sum_+$ so that $H(\lambda, x)$ stands for $H(\lambda, \alpha, Z, P)$. In determining the zeros of H, the following proposition asserts that in a small neighborhood about the optimal at $\lambda=0$, there is a smooth path parameterized by λ consisting of the global optimal solution.

Proposition 4.1: Suppose that $\min J_s(\alpha)$ has a unique global solution α^* satisfying the second order sufficiency condition on the positivity of the

Hessian $[J_s(\alpha^*)]_{,\alpha_i \alpha_j} > 0$. Further, assume that J_s is coercive so that $|J_s(\alpha)| \to \infty$ as $|\alpha| \to \infty$. Then there exists $\epsilon > 0$ such that (3.11) has a unique global solution for $\lambda < \epsilon$.

The next proposition provides a sufficient condition for the path to remain locally optimal.

Proposition 4.2: Let $\phi(\lambda) = (\lambda, x(\lambda))$ denote a smooth path in $[0,r) \times R^{na} \times \sum_+ \times \sum_+$ with $H(\phi(\lambda)) = 0$ and $H_{,x}$ invertible for $\lambda \in [0,r)$. Such an r is guaranteed by Proposition 4.1. Then $\alpha(\lambda)$ is a local minimum for J_λ for each $\lambda \in [0,r)$.

The purpose of the following lemma is to demonstrate that the zero set of H is "generically" well-behaved.

Lemma 4.3: Suppose that $H(0,x)=0$ has a unique solution. Then for almost every choice of $(\nu, V, D_1) \in R^{na} \times \sum_+ \times \sum_+$, the solution path emanating from $(0, x^*)$ is diffeomorphic to the real **R** and every other component of $H^{-1}(o)$ is diffeomorphic to either a circle or **R**.

Thus, following the path defined by one of the zero curves of H, not just the one emanating from the optimal at $\lambda=0$, will not lead to a pathological behavior such as bifurcations or curves with infinite length in bounded sets. Another fundamental and generally difficult question that arises when employing homotopy methods is whether or not the path remains bounded. The following result provides a partial answer to this question.

Proposition 4.4: Suppose that J_s, B_i, D_o, and A are all polynomials in $\alpha_1, \ldots \alpha_{na}$, and assume coercivity of $J_s(\alpha)/|\alpha|$. If $H(0,x)=0$ has a unique solution, then for any $\epsilon > 0$ and for almost every triple $(\nu, V, D_1) \in R^{na} \times \sum_+ \times \sum_+$, the component of $H^{-1}(0)$ containing $(0,x^*)$ is a bounded set in $[0,1-\epsilon] \times R^{na} \times \sum_+ \times \sum_+$.

5. NUMERICAL RESULTS

The numerical experiments described in this section demonstrate the results of the foregoing theory. Two prototype examples are used; both employing the LQR formulation. Implementation of the homotopy strategy of the previous section is achieved by iterative optimization, wherein the solution path for minimizing (3.11) in terms of the homotopy parameter λ starts at $\lambda=0$ with $\alpha_1, \ldots, \alpha_{na}$ initialized to a predetermined sufficiently small allowable size α_o. At this point in the solution space, J_λ is fully weighted toward minimizing J_s only. Minimization of $J_{\lambda o}$ thus yields α_o^* for which $H(\lambda_o, x_o^*)=0$. For the next iteration and for every succeeding one, λ is incremented and the weighting is shifted gradually toward J_c. For a typical iteration j, the following steps are performed:

(i) $\lambda_j \leftarrow \lambda_{j-1} + \Delta\lambda_{j-1}$

(ii) Initialize the minimization of $J_{\lambda j}$ by using $\alpha_j \leftarrow \alpha^*_{j-1}$. This will result in α_j^* for which conditions (3.12) hold.

In performing the minimization in (ii) above, we employed the Automated Design Synthesis (ADS) system of general purpose subroutines [10]. ADS provides a wide selection of options at three levels: strategy, optimization, and line search. Available strategies include sequential linear and quadratic programming, and sequential unconstrained minimization coupled with various penalty methods. At the optimization level, one can choose between Fletcher-Reeves algorithm and the variable metric method of Broydon-Fletcher-Goldfarb-Shanno (BFGS) for unconstrained minimization, or Zoutendijk's method of feasible directions and modifications thereof for constrained minimization. For one-dimensional line search, the options include a combination of polynomial interpolation/extrapolation, solution bounding, and the method of Golden Section. Not all combination of options are compatible at the three levels, and the program parameters must be adjusted to suit the problem at hand. For this purpose, an analytical function was contrived which possessed such features as: easy to compute closed form solution, multiple minima, and insensitivity of the functions gradient near the minima to design parameters. Several compatible options were tried and the program parameter values (e.g., move limits and convergence criteria on the absolute and relative changes in objective function between two successive iterations) were adjusted until the closed form and numerical solution agreed within as few iterations as possible. As a result of these numerical experiments, the popular BFGS variable metric method for unconstrained minimization emerged as the one of choice for use in the combined control-structure optimization examples that follow. During the one dimensional line search, the minimum is located by first computing the bounds, then using polynomial interpolation.

Example 1: The cantilever beam of Fig. 1 resembling a flexible appendage of a large structure is modelled by three finite elements with two degrees-of-freedom (dof) at each node. The structural design variables are the x-sectional areas α_1, α_2, α_3 of the elements. The disturbance v represents a transverse sound pressure modelled by uncorrelated unit impulses at t=0 concentrated at the three nodal transverse dof. The control force u is applied at the free end along the transverse dof direction. With the J_s given by (3.4), we seek the minimum of (3.11) for $\lambda\epsilon[0,1]$, subject to conditions (3.12). Here, the weighting matrices were taken as $D=10^2$ x diag(K,M), and $R=10^{-4}$, and the initial α_i used were $\alpha_i=\alpha_o=1x10^{-7}$, i=1,...,3.

Table 1 lists the family of Pareto optimal designs α_i^* that minimize J_λ, $\lambda\epsilon[0,.99]$ along with the corresponding values for J_c, J_s and J_λ. The variations of the Pareto optimal $J_c^*(\lambda)$, $J_s^*(\lambda)$ and $J_\lambda^*(\lambda)$ are shown in Fig. 2. A number of observations can be made from Table 1 and Fig. 2:

(i) The noncommensurate nature of the two costs J_c and J_s is apparent as the weight is shifted between them: while J_c is a strictly decreasing function of λ, J_s is a strictly increasing function of λ. This is consistent since a stiffer structure requires less control energy.

(ii) Except near $\lambda=0$, the optimal structural shapes that minimize J_λ for the disturbance, choice of D and R, and control forces described above are essentially $\alpha_1=\alpha_2$ near the fixed end, and a much smaller α_3 near the free end. This is a physically plausible optimum shape that minimizes the mixture of high strain energy density near the fixed end and high kinetic energy density near the free end. Other choices of disturbance, control location and D, R are expected to alter the optimal beam shape.

(iii) Although the design at λ=0 is guaranteed to be globally optimal (Proposition 4.1), it is possible that designs generated as λ is continued may be only locally optimal. To assess this possibility, the optimal designs listed for λ=.200, λ=.700 and λ=.900 were re-examined separately. For each case, the minimization was restarted with randomly selected initial α_i values. In most cases, the minimization converged to the same or to a higher minimum than obtained in Table. 1.

Table 1. Pareto Optimal Designs of Example 1

λ	Optimal Design x10^{-3} α_1	α_2	α_3	J_c	J_s	J_λ
0.0	.00010	.00010	.00010	350000.	.007	.007
.000001	.00035	.00038	.00032	96000.	.026	.122
.00001	.00116	.00114	.00077	30800.	.076	.384
.0001	.00570	.00625	.00287	5870.	.369	.955
.005	.0585	.0708	.0187	495.	3.68	6.14
.010	.0801	.0802	.0212	391.	4.52	8.89
.020	.113	.111	.0300	265.	6.33	11.52
.040	.159	.155	.0438	177.	8.90	15.64
.100	.237	.249	.0761	102.	14.00	22.77
.200	.367	.349	.112	61.8	20.62	28.86
.300	.425	.457	.154	46.1	25.80	31.92
.400	.563	.532	.189	35.50	31.97	32.99
.500	.622	.650	.231	27.93	37.43	32.68
.600	.795	.751	.279	21.33	45.45	30.97
.700	.886	.934	.346	16.86	53.92	27.98
.800	1.20	1.14	.44	11.78	69.39	23.30
.900	1.68	1.59	.62	7.30	96.98	16.27
.940	1.93	2.07	.82	5.40	119.9	12.27
.980	3.37	3.22	1.37	2.58	198.2	6.49
.990	3.95	4.40	1.81	1.81	253.6	4.33

Example 2: The beam in this example (See Fig. 3) simulates a flexible appendage (length = 45 m) attached to a rigid hub (inertia = 50 kg.m^2) to which a control torque is applied to counteract the transverse unit impulse at the free end. The beam is modelled by three finite elements of constant width = .001 m, but whose nodal depths $d_1,\ldots,d_4$ represent design variables having a lower bound = .001 m. Here again, J_s represents the total mass of the flexible beam (excluding the hub). For the control objective J_c, the response energy is weighed by D_1 so as to minimize the transverse free end displacement, and R is taken = 1.x10^{-4}.

Table 2 and Fig. 4 represent analogous results to those presented for Example 1 in Table 1 and Fig. 2. In addition to observation (i) of the previous example - which holds here as well - the following remarks can be made with reference to the results of this example:

(i) For small values of λ (e.g. λ=0.1), where the total mass J_s dominates the minimization of J_λ, the optimal shapes tend to have a small slope from $d_1 \rightarrow d_2 \rightarrow d_3$, followed by a sharper slope from $d_3 \rightarrow d_4$. As λ increases, minimizing J_s becomes less important than minimizing J_c (tip displacement response energy plus control energy). As a result, the beam becomes gradually stiffer, and the monotonic slope from $d_1 \rightarrow d_2 \rightarrow d_3 \rightarrow d_4$ associated with small λ values gradually disappears at $\lambda \simeq .45$, then gives way to a pronounced inflection of slope for $d_3 \rightarrow d_4$ for $\lambda > .45$. This results in a larger allocation of mass at the tip. This type of shape is physically consistent with the requirements of the two parts of the control objective J_c: a stiffer structure near the hub that is reduced toward the tip (free end) makes best distribution of mass, while minimizing the tip displacement response. On the other hand, a large mass at the tip (where the disturbance exists) makes the disturbance less effective - thus requiring less control effort.

(ii) To confirm the above interpretation, the case of λ=0.7 in Table 2 (i.e. $R=10^{-4}$) was re-examined for smaller and larger values of R; $R=10^{-6}$ and $R=10^{-2}$, respectively. As Fig. 5 shows, smaller values of R give more weighting to the tip displacement response energy part of J_c, thus giving rise to the optimum shape being a stiffer structure near the hub which is reduced toward the tip. Conversely, larger values of R (e.g. $R=10^{-2}$) give more relative weighting to the control energy part of J_c, which is best minimized by the presence of the heavier tip mass. It is interesting to note the similar effect of varying R and varying λ on the optimal shapes.

Table 2. Pareto Optimal Designs for Example 2.

λ	Optimum Design d_1	d2	d_3	d_4	J_c	J_s	J_λ
.000	.001	.001	.001	.001	$1.6 \times 10^{+10}$	.075	.075
.0001	.02404	.02363	.02291	.01366	3355.26	1.628	1.963
.001	.03552	.03485	.03359	.02065	482.6	2.404	2.884
.010	.05223	.05134	.04940	.03043	70.78	3.54	4.21
.100	.07699	.07559	.07157	.05303	10.03	5.28	5.757
.200	.08759	.08563	.08031	.06659	5.33	6.05	5.906
.300	.09550	.09267	.08657	.07847	3.54	6.62	5.703
.400	.10258	.09867	.09187	.09085	2.56	7.15	5.31
.500	.10944	.10389	.09670	.10470	1.93	7.66	4.79
.600	.11715	.10948	.10135	.12176	1.46	8.22	4.17
.700	.12657	.11576	.10681	.14516	1.08	8.92	3.43
.800	.13944	.12322	.11304	.18055	.77	9.87	2.59
.900	.16369	.13641	.12430	.24923	.47	11.63	1.59
.920	.17299	.14104	.12893	.27374	.41	12.28	1.355
.940	.18542	.14815	.13565	.30544	.34	13.18	1.107
.960	.20578	.16117	.14818	.35131	.26	14.64	0.83
.980	.25035	.19468	.18421	.42401	.16	17.83	0.52
.990	.29401	.25488	.24878	.48165	.09	22.20	0.32

(iii) Of general interest to problems in combined optimization - at least numerically - is the question as to the degree of "roughness" of the hyper-surface $J_\lambda(\alpha)$. A partial answer to this question is provided in Fig. 6 after introducing idealizations that reduce the number of variables from four $(d_1,\ldots,d_4)$ to only two (d_3, d_4), so that a three dimensional plot could be generated. Figure 6 shows such a surface in the neighborhood of the optimum for the case λ=0.7 in Table 2. This is achieved by fixing d_1=.13, allowing d_3 and d_4 to assume various values larger and smaller than those in Table 2 for λ=0.7, and letting d_2=½(d_1+d_3). Assuming that the idealizations above (which led to reducing the dimensionality of the J_λ surface) did not alter the basic topology of J_λ surface, it appears from Fig. 6 that J_λ is a smooth function of the design variables - at least in the neighborhood of the minimum. Furthermore, with these idealizations it appears that J_λ is relatively flat near the minimum along the d_4 axis, and that the optimum shape is some linear combination of the four basic shapes depicted at the corners.

6. CONCLUSIONS

An approach for combined control-structure optimization keyed to enhancing early design trade-offs has been outlined and illustrated by numerical examples. The approach employs a homotopic strategy and appears to be effective for generating families of designs that can be used in these early trade studies.

Analytical results were obtained for classes of structure/control objectives with LQG and LQR costs. For these, we have demonstrated that global optima can be computed for small values of the homotopy parameter. Conditions for local optima along the homotopy path were also given. Details of two numerical examples employing the LQR control cost were given showing variations of the optimal design variables along the homotopy path. The results of the second example suggest that introducing a second homotopy parameter relating the two parts of the control index in the LQG/LQR formulation might serve to enlarge the family of Pareto optima, but its effect on modifying the optimal structural shapes may be analogous to the original parameter λ.

ACKNOWLEDGEMENT

The research described in this paper was performed as part of the Control Structure Interaction (CSI) Program at the Jet Propulsion Laboratory, California Institute of Technology, under contract with the National Aeronautics and Space Administration.

REFERENCES

1. D. S. Bodder and L. Junkins, "Eigenvalue Optimization Algorithms for Structural/Control Design Iterations," Amer. Contr. Conf., San Diego, CA, June, 1984.

2. K. Lim and J. Junkins, "Robust Optimization of Structural and Controller Parameters," Journal of Guidance, Vol. 12, January, 1989, pp. 89-96.

3. N. S. Khot, F. E. Eastep, and V. B. Venkaya, "Simultaneous Optimal Structural/Control Modifications to Enhance the Vibration Control of a Large Flexible Structure," Proc. of the AIAA Guid., Nav. and Contr. Conf., 1985, pp. 459-466.

4. S. K. Morrison, Y. Ye, C. F. Gregory, Jr., R. Kosut, and M. E. Regelbrugge, "Integrated Structural/Controller Optimization for Large Space Structures," AIAA Guid. and Contr. Conf., Minneapolis, MN, 1988.

5. M. Salama, J. Garba, and F. Udwadia, "Simultaneous Optimization of Controlled Structures," Journal of Computational Mechanics, Vol. 3, 1988, pp. 275-282.

6. M. Milman, R. Scheid, M. Salama, and R. Bruno, "Methods for Combined Control-Structure Optimization," Proceedings of the VPI Symposium on the Dynamics and Control of Large Structures, Blacksburg, VA, May, 1989.

7. J. G. Lin, "Maximal Vectors and Multi-Objective Optimization," Journal of Opt. Theory and Appl., Vol. 18, January, 1976, pp. 41-65.

8. H. Kwakernaak and R. Sivan, "Linear Optimal Control System," Wiley Inter-Science, NY, 1972.

9. M. Milman, M. Salama, R. Scheid, R. Bruno, and S. Gibson, "Integrated Control-Structure Design: A Multiobjective Approach," JPL Report D-6767, (internal report), October, 1989.

10. G. Vanderplaats, "ADS - A Fortran Program for Automated Design Synthesis," NASA CR-172460, October, 1984.

Figure 1

EXAMPLE 1.
CANTILEVER BEAM PROBLEM

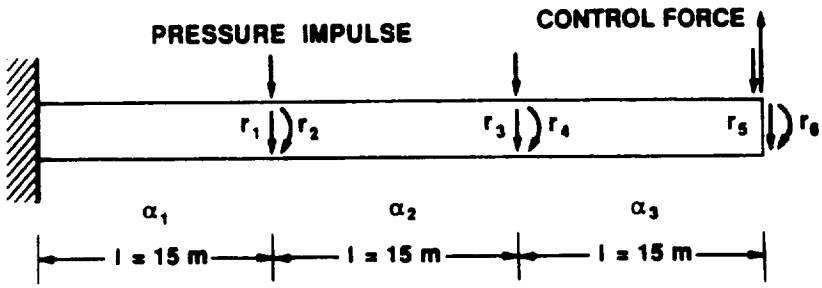

STRUCTURAL MODEL: MASS DENSITY = 1660 Kg/m^3, MODULUS = 9.56 x 10^{10} N/m^2
MODAL DAMPING = 0.5%

CONTROL: DISTURBANCE = TRANSVERSE PRESSURE IMPULSE CONCENTRATED AT THE NODES
RESPONSE ENERGY WEIGHTED BY $\tilde{D}$ = Diag (K,M) x 10^2,
CONTROL ENERGY WEIGHTED BY R = 1 x 10^{-4}

DESIGN VARIABLES: $\alpha_1, \alpha_2, \alpha_3 \geq 1 \times 10^{-7}$

Figure 2

CANTILEVER BEAM OPTIMIZATION

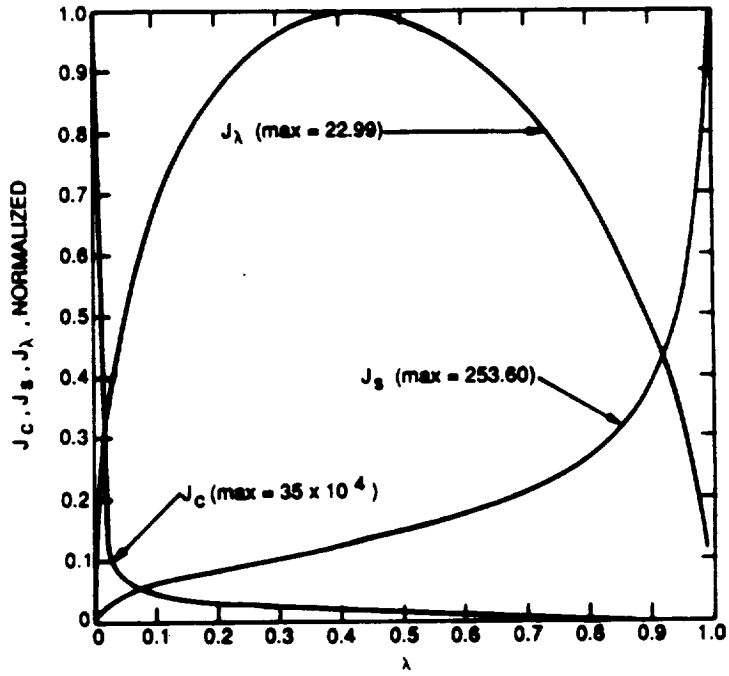

Figure 3

EXAMPLE 2.
HUB-BEAM PROBLEM

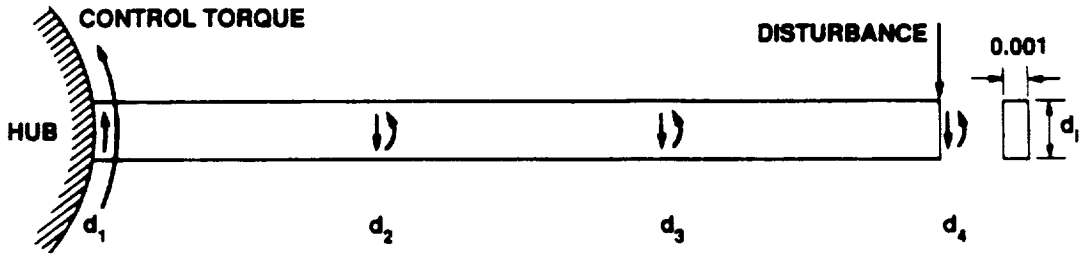

STRUCTURAL MODEL: MASS DENSITY = 1660 Kg/m^3, MODULUS = 9.56 x 10^{10} N/m^2
MODAL DAMPING = 0.5%,

CONTROL: DISTURBANCE = UNIT IMPULSE
RESPONSE ENERGY WEIGHTED TO MINIMIZE END DISPLACEMENT, R = 1 x 10^{-4}

DESIGN VARIABLES: $d_1, \cdots, d_4 \geq 0.001$

Figure 4

HUB-BEAM OPTIMIZATION

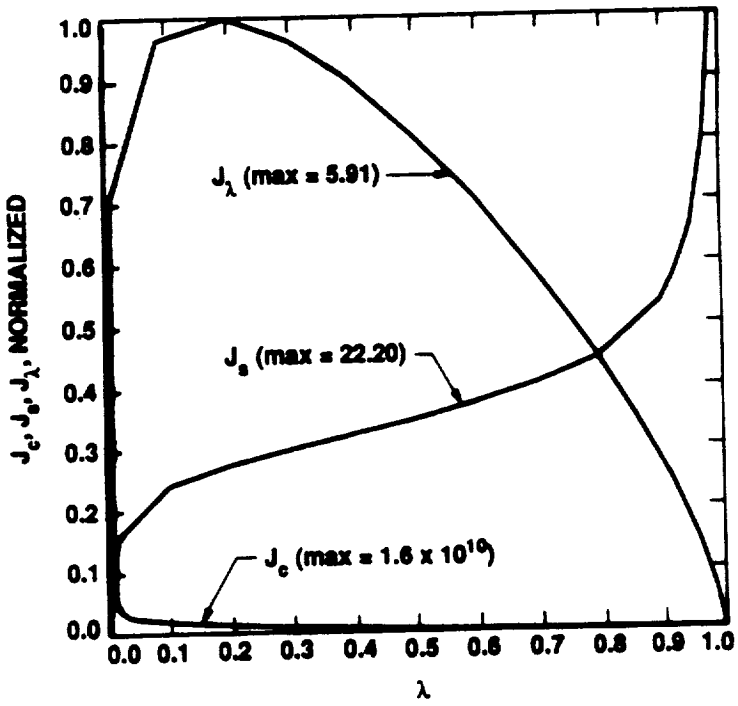

Figure 5

OPTIMUM SHAPES

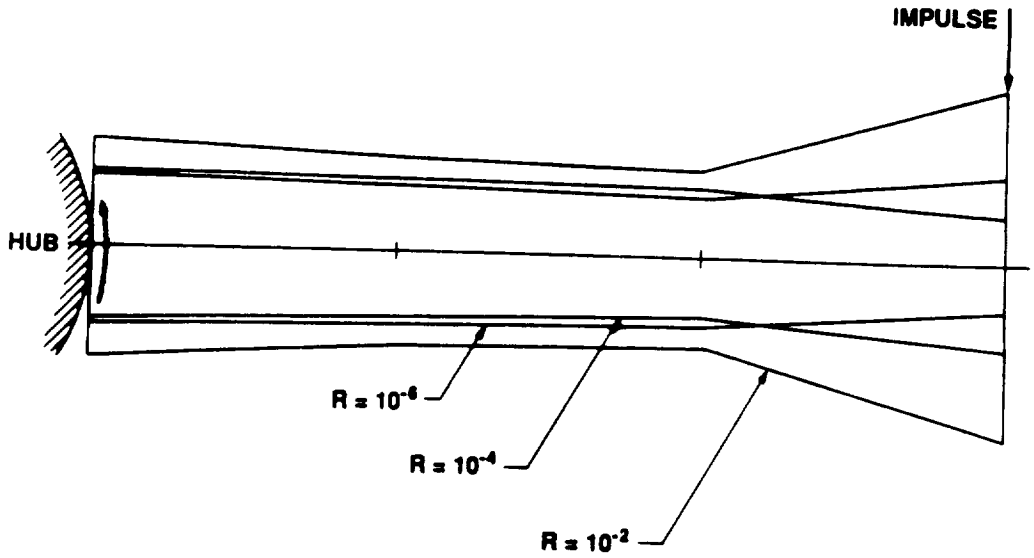

Figure 6

$J_\lambda(d_3,d_4)$ SURFACE NEAR THE MINIMUM, $\lambda = 0.7$